ORIGINAL PAPER

On the Photophysical Properties of New Luminol Derivatives and their Synthetic Phthalimide Precursors

Raúl Pérez-Ruiz · Robert Fichtler · Yrene Diaz Miara · Matthieu Nicoul · Dominik Schaniel · Helfried Neumann · Matthias Beller · Dirk Blunk · Axel G. Griesbeck · Axel Jacobi von Wangelin

Abstract The photophysical properties of a series of structurally related 4-aminophthalimides and the corresponding 5-aminophthalic hydrazides (luminols) are reported. Absorption, steady-state, and time-resolved fluorescence spectra of luminols exhibited substitution, solvent, and pH dependence. Singlet lifetimes have been determined by time-resolved laser flash spectroscopy. UV spectra in gas phase and DMSO solution were calculated by TD-DFT which revealed the existence of two low-energy excited singlet states with strong pH-sensitivity.

Keywords Fluorescence · Luminols · Phthalimides · Singlet lifetime · pH dependence

R. Pérez-Ruiz · R. Fichtler · Y. Diaz Miara · D. Blunk · A. G. Griesbeck (✉) · A. Jacobi von Wangelin (✉)
Department of Chemistry, University of Cologne, Greinstr. 4,
50939 Köln, Germany
e-mail: griesbeck@uni-koeln.de
e-mail: axel.jacobi@uni-koeln.de

D. Blunk
e-mail: d.blunk@uni-koeln.de

M. Nicoul · D. Schaniel
Department of Physics I, University of Cologne,
Zülpicher Str. 77,
50937 Köln, Germany

H. Neumann · M. Beller
Leibniz-Institute of Catalysis,
Albert-Einstein-Str. 29a,
18059 Rostock, Germany

Introduction

Aromatic molecules with both electron-donating and electron-accepting substituents (**I**) have been intensively investigated for their special photophysical properties which distinguish them from simple donor or acceptor-substituted arenes (Scheme 1) [1]. Among them, phthalimide derivatives (**II**) play an important role with diverse applications as dyes, brighteners, bioactive drugs, biomarkers, or photocatalysts [2]. Aminophthalic hydrazides (**III**) belong to a related class of compounds that display unique photophysical and photochemical properties but are still on an infant stage with regard to applications. The parent molecule luminol, 5-amino-2,3-dihydrophthalazine-1,4-dione, has been known for decades for its robust chemiluminescence (CL) in the presence of oxidants, which led to practical applications as analytical probe for metal ions, oxidants, or anions [3]. Spectroscopic properties of luminol, particularly its fluorescence behavior, have been the subject of numerous investigations due to its intense solvent-dependent emission and pronounced Stokes shifts. Mukherjee and co-workers [4] studied the lowest excited singlet state of luminol which exhibits a red-shifted emission in protic solvents. Recently, Vasilescu and co-workers [5] performed a spectroscopic study of luminol in dimethyl sulfoxide (DMSO), DMSO-water and alkaline DMSO-water showing a reversible acid-base equilibrium with distinct fluorescence behaviour.

While numerous studies have been performed with luminol and simple mono-substituted luminol derivatives, only a handful of higher substituted compounds have been investigated. Structural variations were carefully studied by Brundrett and White [6], who investigated the influence of the luminol constitution on its CL behavior. Subsequently, White and Bursey [7] observed a beneficial effect on the

Scheme 1 Push-pull arenes as model systems for photophysical studies

I
Donor-Acceptor-Arenes

II
Phthalimides

III
Phthalic Hydrazides (= Luminols)
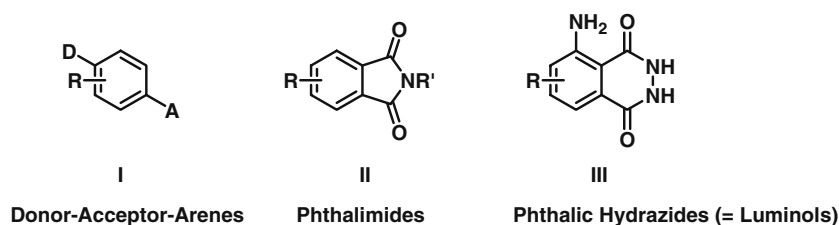
CL quantum yield by methoxy substitution. Brundrett and White [8] and Gundermann and Drawert [9] showed that luminols bearing 6-alkyl substituents display enhanced excited state formation and thus increased CL. Detailed investigations of structure-activity (CL) relationships have been limited by the lack of reliable synthetic procedures toward new luminol derivatives. To address this bottleneck of synthetic access to new derivatives especially with multiple substituents, we developed a practical three-step synthesis of luminol derivatives based upon commercially available starting materials [10], which is part of a wider research program directed at practical one-pot procedures for the efficient synthesis of diversified carbocyclic and heterocyclic building blocks [11]. Herein, we wish to report on the detailed investigation of the photophysical properties of a series of phthalimides and the corresponding luminol derivatives. The study involves absorption and fluorescence spectra in DMSO and aqueous buffer solutions at different pH, the determination of singlet state lifetimes, DFT calculations of UV spectra in gas phase and solution, and a discussion of electronic and steric substitution effects.

Experimental section

Materials

The synthesis of phthalimides **9**–**16** was realized from commercial starting materials via sequential thermal cyclo-addition and palladium-catalyzed transfer hydrogenation on 30 mmol scales [10]. Simple hydrazinolysis of phthalimides gave the corresponding phthalic hydrazides **17**–**24** as colourless to off-white solids [10]. All products were isolated and purified by silica gel flash chromatography.

Absorption spectroscopy

Absorption spectra were recorded on a Beckman Coulter UV-DU800. Samples were placed into quartz cells of 1 cm path length. All concentrations were 10^{-4} M.

Steady-state fluorescence

Emission and excitation spectra were carried out using a Perkin-Elmer LS-50B luminescence spectrometer. Samples

were placed into quartz cells of 1 cm path length. Concentrations were fixed as indicated in the text.

Time-resolved fluorescence

Singlet lifetime measurements were performed after excitation with laser pulses of 120 fs length. The pump laser was an "Integra-C" from Quantronix providing pulses of 2 mJ with 160 fs duration at 796 nm and 500 Hz repetition rate. Pulses of 1.4 mJ were sent to an Optical Parametric Amplifier "TOPAS" from Light Conversion. The OPA was set to deliver pulses of 355 nm wavelength. The laser repetition rate was reduced to 50 Hz with the use of a chopper. The UV pulses were then focused with a 10 cm focal lens onto the solution under investigation. The sample was placed slightly before the focus to avoid bubble formation, the concentration of the probe was adjusted to exhibit complete absorption of the UV pulse and give light emission in a small region behind the quartz window. The emitted light was collected with a lens and sent onto an ultra-fast photodiode (2 GHz bandwidth). A color filter was placed before the diode to ensure that no reflected or scattered light from the pump pulse impinged on the detector. The spectral traces of the ultra-fast diode were recorded on a WavePro 960XL oscilloscope from LeCroy (2 GHz bandwidth). Each trace was the average of 1000 single traces.

DFT calculations

All density functional theory (DFT) calculations were performed with the Becke three parameter hybrid functional [12] with the correlation functional of Lee, Yang, and Parr (B3LYP) [13] and applying the 6-311++G(d,p) [14] basis set as implemented in the Gaussian 03 program suite [15] applying an ultrafine integration grid (99,590). Each geometry optimization was performed under tight optimization convergence criteria. For each of the optimized structures the analytical Hessian was calculated (vibrational analysis) to ensure the absence of any negative Eigen values and thus to ascertain the minimum character of the stationary state. Bulk solvent effects were taken into account by applying a polarizable continuum model (PCM) [16] with dimethyl sulfoxide parameters. For the cavity generation, the radii from the UFF force field with
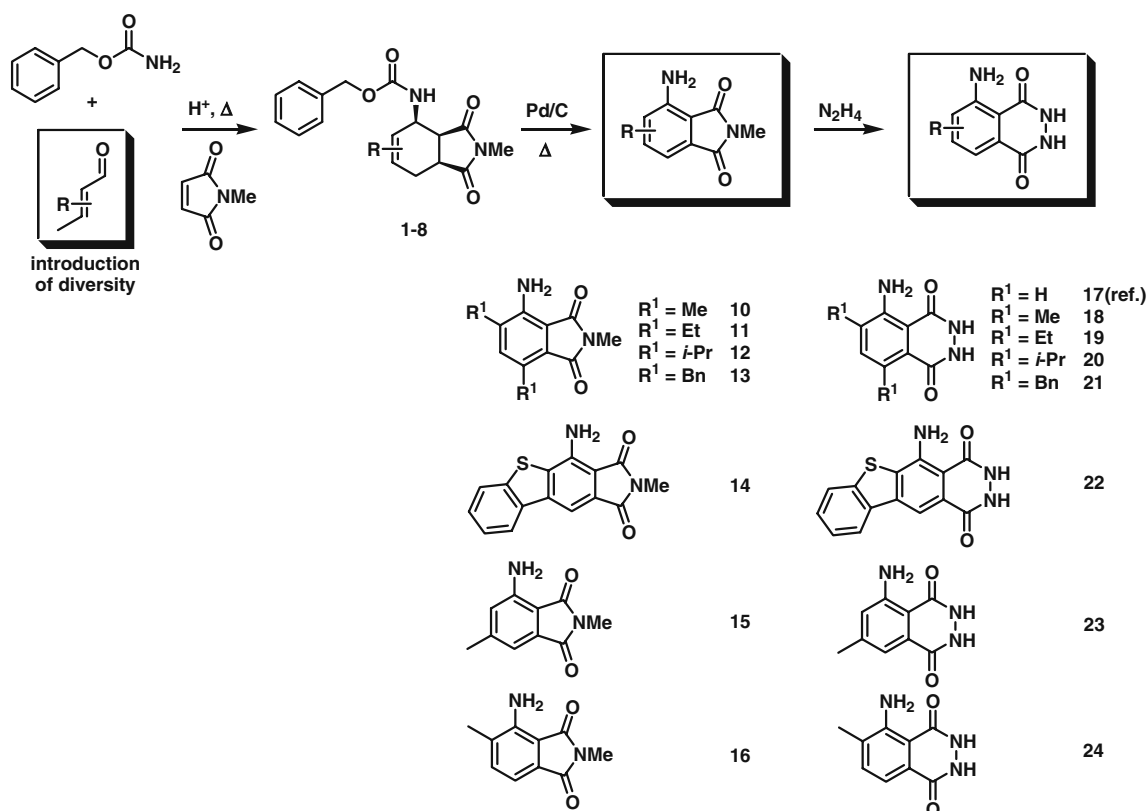
Scheme 2 Synthesis of phthalimide and luminol derivatives (parent luminol **17** as reference)

individual spheres at the hydrogens have been applied. The UV-vis spectra were computed for the optimized structures by calculating the first 10 excited singlet states with time-dependent density functional theory (TD-DFT) [17].

Results and discussion

Synthesis of phthalimide and luminol derivatives

The synthesis of phthalic hydrazide derivatives **17–24** involved a three-step sequence: 1) acid-catalyzed three-

component coupling of *O*-benzyl carbamate with the corresponding unsaturated aldehyde and *N*-methyl maleimide afforded the Cbz-protected aminocyclohexenes **1–8** [10a,10b,11]; 2) thermal treatment in the presence of catalytic amounts of palladium-on-charcoal resulted in deprotection of the amine function and concomitant oxidation of the

Table 1 Absorption (abs) and emission (em) properties of phthalimides **10–16**

Compound	λ_{abs} (nm)[a]	ε[a]	λ_{em} (nm)[b]	$\Delta\lambda$ (cm^{-1})[c]
10	397	5712	470	3912
11	400	6306	475	3948
12	401	6124	472	3751
13	401	5520	475	3885
14	404	5909	454	2726
15	393	5302	466	3986
16	390	5170	460	3902

[a] $c=10^{-4}$ M; [b] $c=3.3\cdot10^{-6}$ M; [c] Stokes shift

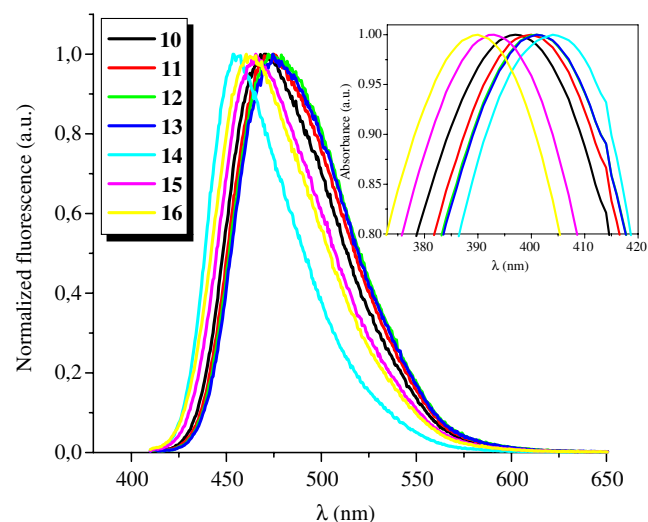**Fig. 1** Normalized fluorescence spectra ($\lambda_{ex}=400$ nm) of phthalimides **10–16** in DMSO under aerobic conditions; $c=3.3\cdot10^{-6}$ M. Inset: Normalized absorption spectra of **10–16** in DMSO; $c=10^{-4}$ M
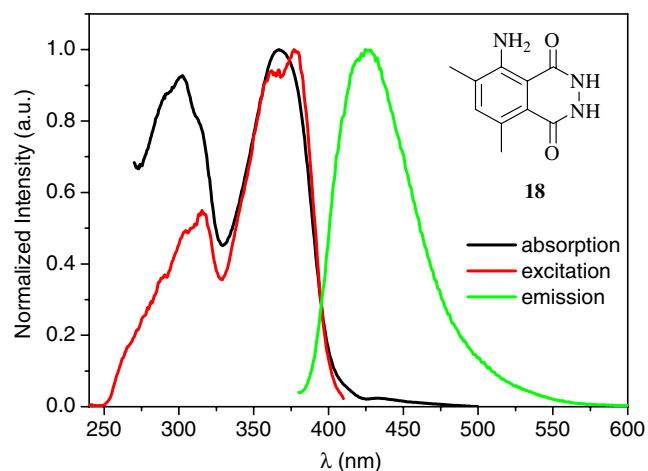
Table 2 Spectral properties of **17**–**24**: absorption (abs) and emission (em) maxima and Stokes shifts

Compound	λ_{abs} (nm)[a]	ε[a]	λ_{em} (nm)[b]	$\Delta\lambda$ (cm^{-1})[c]
17	297	7768		
	358	7508	405	3241
18	302	8972		
	367	9676	425	3718
19	305	5872		
	368	7752	429	3863
20	304	6232		
	370	8196	430	3771
21	305	9320		
	372	10016	430	3625
22	333	9048		
	380	9852	418	2392
	398	10152	435	
23	297	8176		
	358	8304	401	2995
24	297	6156		
	357	7916	408	3501

[a] c=2.5·10^{-5} M; [b] c=2.5·10^{-6} M; [c] Stokes shift

Table 3 Singlet state and fluorescence data of luminol derivatives in DMSO

Luminol	E_S (kcal/mol)[a]	τ_S (ns)	Φ_F[b]	$k_F \cdot 10^8$ (s^{-1})[c]
17	75	1.8[c]	0.15	0.8
18	72	2.0	0.23	1.1
19	72	2.0	0.21	1.0
20	72	2.0	0.31	1.5
21	72	2.2	0.48	2.1
22	70	0.9	0.21	2.3
23	75	2.8	0.40	1.4
24	75	1.8	0.34	1.8

[a] Singlet energy; [b] fluorescence quantum yield (for luminol, Φ_F=0.15, see ref. [5]; [c] fluorescence rate constant, $k_F = \phi_F / \tau_S$

higher ring strain and reduced mesomeric delocalization of the amide moiety, phthalimides **10**–**16** exhibit higher stretching frequencies of the carbonyl bands (1755–1680 cm^{-1}) in the characteristic IR region than the six-membered phthalic hydrazides **17**–**24** (1675–1589 cm^{-1}).

Spectral properties of phthalimides

The absorption spectra of DMSO solutions of phthalimides **10**–**16** show a single maximum in the 390–404 nm range (Table 1, Fig. 1 inset). The fluorescence spectra of **10**–**16** were recorded with a constant excitation wavelength of λ_{ex}= 400 nm under aerobic conditions (Fig. 1). Emission maxima appeared between 454 and 475 nm, benzothiophene derivative **14** exhibited the most blue-shifted fluorescence at 454 nm. The lowest singlet energies were determined from the absorption/emission spectra overlap as 65–66 kcal/mol
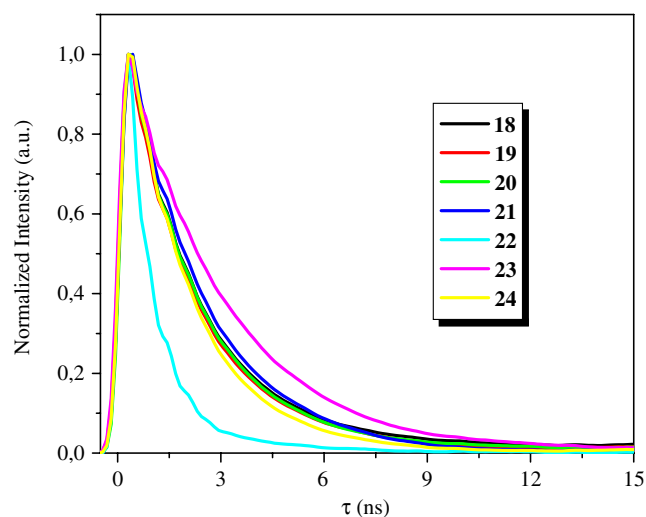
cyclohexene ring in one operation [10d]; 3) subsequent hydrazinolysis gave the luminol derivatives (**17**–**24**) as air stable solids in good yields [10e] (Scheme 2).

From a practical standpoint it is important to note that all starting materials and reagents for the synthesis of **17**–**24** are commercially available. The procedure has been optimized to allow for the preparation of luminols on multi-gram scales. The reactions can be performed in standard glassware without resorting to oxygen/moisture-free conditions. The overall yields over three synthetic steps were in the range of 31–62 %. As a consequence of the

Fig. 2 Normalized absorption, excitation, and emission spectra of **18** in DMSO; c=2.5·10^{-6} M

Fig. 3 Normalized fluorescence decays (λ_{ex}=355 nm) of luminols **18**–**24** in DMSO under aerobic conditions; c=1.3·10^{-3} M

Table 4 Spectroscopic data in aqueous buffer solutions (10 vol% DMSO) at different pH

	pH3			pH7			pH12
	λ_{abs}	λ_{em}	$\Delta\lambda^a$	λ_{abs}	λ_{em}	$\Delta\lambda^a$	λ_{abs}
17	294, 351	430	5234	301, 351	–	–	301, 351
18	301, 360	443	5240	309, 356	443	5516	312, 354
19	303, 360	446	5356	311, 357	446	5589	316, 357
20	304, 362	450	5402	313, 359	450	5632	317, 357
21	–	–	–	–	–	–	317, 362
22	–	–	–	322, 337, 381	437, 492	3294, 5852	322, 337, 381
23	296, 350	428	5206	303, 347	427	5399	303, 347
24	294, 351	431	5288	304, 349	429	5343	305, 349

All λ values in nm; c= $1.5\cdot10^{-4}$ M (λ_{abs}); c= $2.5\cdot10^{-6}$ M (λ_{em}); λ_{ex}=350 nm (380 nm for **22**); [a] Stokes shift in cm^{-1}.

for all phthalimides. Moderate Stokes shifts were observed from the difference of absorption and emission maxima (Table 1). Comparable values were observed for derivatives **10** (3912 cm^{-1}), **11** (3947 cm^{-1}), **12** (3751 cm^{-1}), **13** (3885 cm^{-1}), **15** (3939 cm^{-1}), and **16** (3901 cm^{-1}). A significantly smaller Stokes shift value was determined for the sulfur-containing derivative **14** (2677 cm^{-1}).

Absorption and steady-state fluorescence of luminol derivatives 17–24

Previous to this study, detailed photophysical data of the parent luminol **17** were determined in DMSO [4, 5] and a series of other solvents [18]. In order to use luminol as reference system and evaluate comparable spectroscopic data, we performed all photophysical measurements in DMSO. Table 2 summarizes the relevant spectral data that were collected for luminol derivatives **18**–**24**. Absorption spectra of **18**–**21**, **23**, and **24** in DMSO exhibited two distinct bands which were comparable to the parent compound **17**, whereas three red-shifted maxima were found for benzothiophene **22**. Concerning peak positions, the excitation spectra completely matched the absorption spectra. The band in the 355–380 nm region was in all cases stronger than the 295–320 nm band. The presence of these two bands in the absorption as well as excitation spectra indicate the presence of two distinct electronically excited states S_1 and S_2. It is thus obvious that excited luminol derivatives relax from the S_2 (π,π^*)-state to the S_1 (π,π^*)-state and, after a possible complex formation with DMSO, emit from the S_1 (π,π^*)-state. For compound **22**, three bands were detected in both, absorption and excitation spectra, all slightly red-shifted in comparison to **17**. The anellated benzothiophene in **22** serves as a strong electron-donating group which, in addition to the two local excited singlet states, might stabilize an internal charge transfer state.

The emission spectra of the luminol derivatives **17**–**21**, **23** and **24** showed broad bands between 405 and 430 nm

(see for example Fig. 2); two separate fluorescence bands were observed for benzothiophene compound **22**. The addition of one methyl group in the donor-acceptor system of parent luminol **17** did not significantly alter the fluorescence properties (see **23** and **24**). Although the *para* orientation of electron-donating methyl substituents and an electron-accepting carbonyl moiety is likely to exert electronic communication across the arene, steric effects appear to be more dominant. The introduction of 6,8-disubstitution in **18**, **19**, **20** and **21** and anellation with benzothiophene (**22**) prompted moderate red-shifts of the emission band ($\Delta\lambda_{em}$=20–25 nm) in comparison with **17**. Although this might be a direct consequence of the electron-donor abilities of the substituents and facilitate the formation of an internal charge transfer state after local excitation to S_1, we postulate a pivotal steric effect induced by two substituents in *ortho*-positions to the amino and carbonyl groups of the parent luminol system. This could directly affect the geometry of the excited states and thus influence their energy and lifetime [18]. Moderate Stokes
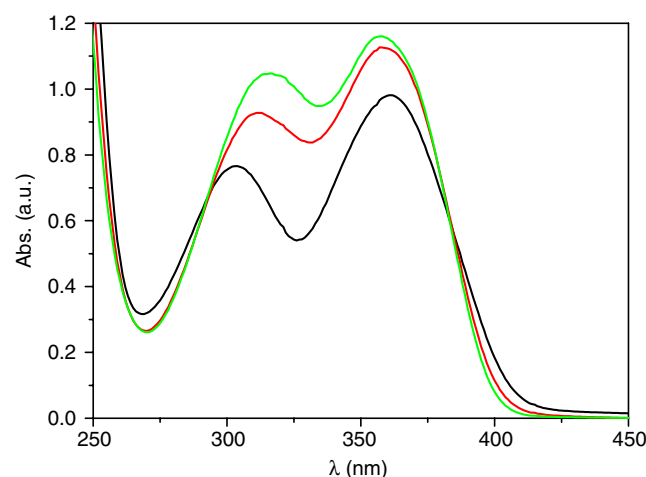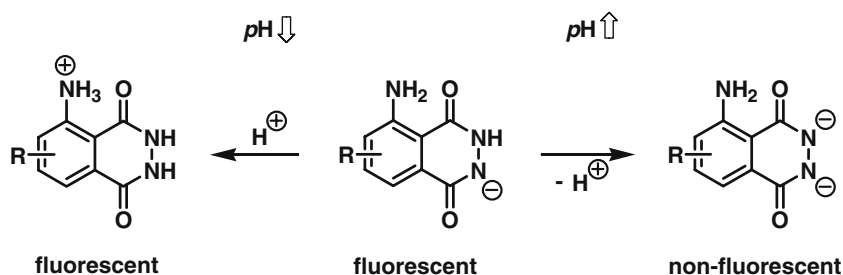

Fig. 4 Normalized absorption spectra of **19** in H$_2$O/DMSO (9/1 v/v) at pH3 (—), pH7 (—) and pH12 (—); c=$1.3\cdot10^{-3}$ M

Scheme 3 pH-dependent fluorescence of luminol derivatives

shifts (≥ 3000 cm^{-1}) were determined for all compounds except the sulfur-containing compound **22** (Table 2).

The excited singlet state energies were calculated from the intersection of excitation and emission bands and exhibited no significant dependence on the substitution pattern (Table 3). In contrast to the excited state energies, the fluorescence quantum yields showed significant changes in comparison to luminol **17**. Dibenzyl derivative **21** displayed a more than tripled fluorescence quantum yield (0.48 vs. 0.15 for **17** [5]). The singlet state decay traces of **18**–**24** showed mono-exponential behavior (Fig. 3). As can expected from the significantly smaller Stokes shift, **22** has a shorter singlet state lifetime. This is in full accord with its largest fluorescence rate constant among the luminols studied here.

pH-dependence of absorption and steady-state fluorescence

A recent spectrophotometric study of luminol (**17**) in DMSO, DMSO-water and alkaline DMSO-water showed a pH dependence of its absorption and fluorescence properties [5]. We investigated the photophysical properties of the new luminol derivatives **18**–**24** under identical conditions. Absorption and steady-state fluorescence measurements of luminols **17**–**24** were performed in water at different pH (commercial buffer solutions of pH 3, 7 and 12 with 10 vol% DMSO). As can be seen from Table 4, at least two absorption maxima were found. Benzothiophene derivative **22** exhibited an additional red-shifted absorption band at 381 nm. Poor solubility of **22** (pH 3) and dibenzyl derivative **21** (pH 3 and 7) accounted for the lack of reliable data under these conditions. When increasing the pH, the low-energy transition of diethyl-substituted luminol **19** is subtly blue-shifted and accompanied by a moderate increase of the extinction coefficient (Fig. 4); a much more pronounced effect becomes apparent from the high energy transition that shows a batho- and hyperchromic behavior with increasing pH.

Based on the high acidity of the phthalic hydrazide moiety (pK_a 12.7 in DMSO [19], cf. pK_a of acetic acid in DMSO= 12.6), it can be assumed that the hydrazide is fully deprotonated (dianion stage) at high pH and non-protonated at pH 3. The 5-amino group (aniline) is not subject to deprotonation even at pH 12, however, protonation occurs

Fig. 5 Amino-protonated (upper structure and spectrum) and non-protonated (lower structure and spectrum) phthalic hydrazide **18** calculated by B3LYP/6-311++G(d,p)
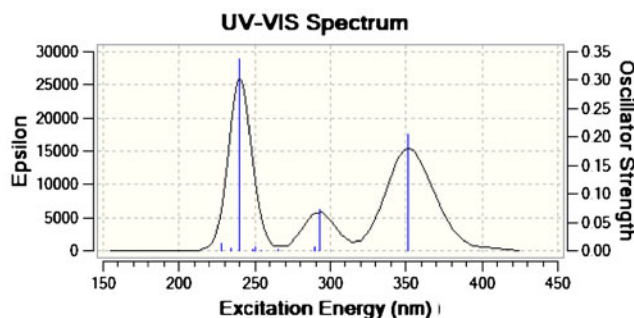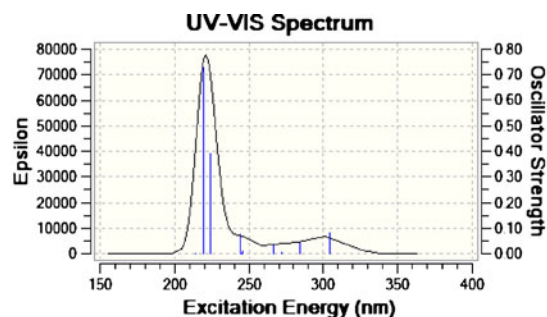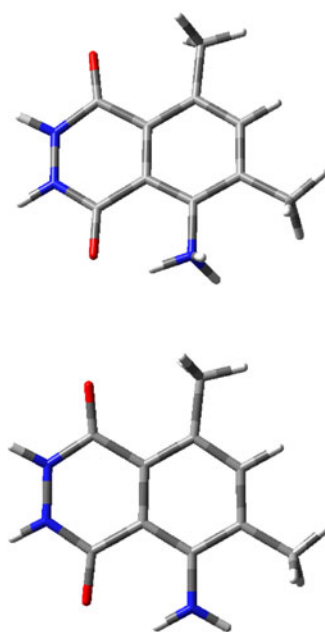
under acidic conditions. Thus, a complex equilibrium between $ArNH_2$, $ArNH_3^+$, hydrazide mono- and dianionic species is operative under various pH conditions (Scheme 3). To make the story even more complicated, theoretical calculations [20] revealed the existence of different tautomers (which is especially important for the neutral and the monoanionic species) that make a detailed analysis of the absorption behavior challenging. The most pronounced changes in absorption are the increased absorption in the long-wavelength region of the UV-vis spectra (between 300 and 350 nm) at increasing pH values coupled with slight absorption shifts. When raising the pH from 3 to neutral, this trend can be correlated with the increasing absorption of the neutral hydrazide portion of the molecule. Identical effects (of different magnitudes) were also detected for luminol derivatives **17**, **18**, **20**, and **21** as well as for the mono-alkylated compounds **23** and **24**, respectively. As expected, strong fluorescence was observed at pH 3 for all derivatives whereas their intensities decreased to ~50% at pH 7. In consistency with literature results [5], no emission of any luminol derivative was detected at pH 12: This is in full agreement with the formation of the dianionic phthalhydrazide species and the delocalization of the negative charges and, consequently, the fluorescence quenching by internal charge transfer. Finally, the increase in Stokes shifts at higher pH can be interpreted as an increased charge shift stabilization of the excited state relative to the ground state.

Theoretical considerations

In order to investigate the background of the pH-dependence of the absorption spectra of luminol derivatives **17**–**21**, the electronic absorption spectra (UV-vis) of the 6,8-dimethyl derivative **18** were calculated in the gas phase and in DMSO environment in the protonated and non-protonated form mimicking the situations at pH=3 and pH=7, respectively. As can be seen in Fig. 5, the absorption spectrum of protonated **18** (resembling low pH) is dominated by a benzene-type transition at 219 nm and several transitions with lower extinctions between 267 and 304 nm. In the non-protonated state (resembling neutral pH), a strong band at 352 nm appeared. The latter transition is the dominating line at $\lambda > 300$ nm for compounds **17** and **18** (see Fig. 4) at high and low pH values. In agreement with the calculations, the experimental extinction coefficients of both red-shifted transitions increase with increasing pH, and the 300 nm absorption is more strongly influenced by such pH shift. Thus, the TD-DFT study clearly supports the assumption of two pH-dependent transitions at about 300 nm and 350 nm and a less sensitive transition at higher energies (<250 nm) which is strongly red-shifted (from 219 nm to 240 nm) when going from low to neutral pH conditions.

Summary

The photophysical properties of a series of substituted phthalimides and their corresponding luminol products were investigated and compared with that of the parent luminol. All compounds were available by facile multi-component reactions from simple starting materials. Detailed spectroscopic data of luminol derivatives **17**–**24** were collected with respect to absorption and fluorescence behaviour. Singlet lifetimes (0.9–2.8 ns, cf. 1.8 ns for luminol **17**) and quantum yields of the fluorescent excited singlet states (0.21–0.48, cf. 0.15 for **17**) were determined in DMSO. Significant differences were detected depending on the substituents in particular for the presence of heterocyclic ring anellation (see benzothiophene **22**). Additionally, the photophysical behavior of luminol derivatives **17**–**24** were studied under different pH conditions in aqueous buffer solutions. The absorption spectra revealed several species with a major presence of the dianionic luminol derivative at pH 12 which exhibited no significant fluorescence. Theoretical calculations support the assumption of a stronger absorbance of the low-energy transitions under acidic and neutral pH conditions.

References

1. Grabowski ZR, Rotkiewicz K, Rettig W (2003) Structural changes accompanying intramolecular electron transfer: Focus on twisted intramolecular charge-transfer states and structures. Chem Rev 103:3899–4031

2. Griesbeck AG, Hoffmann N, Warzecha K-D (2007) Photoinduced-electron-transfer chemistry: from studies on PET processes to applications in natural product synthesis. Acc Chem Res 40:128–140

3. a) Mestre YF, Zamora LL, Calatayud JM (2001) Flow-chemiluminescence: a growing modality of pharmaceutical analysis. Luminescence 16:213–235. b) Lin ZY, Chen JH, Chen GN (2007) Study on the electrochemiluminescent behavior of menadione sodium bisulfite in presence of luminol. Talanta 72:1681–1686. c) Richter MM (2004) Electrochemiluminescence (ECL). Chem Rev 104:3003–3036. d) White EH, Roswell DF (1970) Chemiluminescence of organic hydrazides. Acc Chem Res 3:54–62

4. Mitra S, Das R, Mukherjee S (1995) Complex-formation and photophysical properties of luminol - solvent effects. J Photochem Photobiol A: Chem 87:225–230

5. Vasilescu M, Constantinescu T, Voicescu H, Lemmetyinen H, Vuorimaa E (2003) Spectrophotometric study of luminol in dimethyl sulfoxide-potassium hydroxide. J Fluorescence 13:315–322

6. Brundrett RB, White EH (1974) Synthesis and chemilumines-cence of derivatives of luminol and isoluminol. J Am Chem Soc 96:7497–7502

7. White EH, Bursey MM (1966) Analogs of luminol. Synthesis and chemiluminescence of two methoxy-substituted aminophthalic hydrazides. J Org Chem 31:1912–1917

8. Brundrett RB, Roswell DF, White EH (1972) Yields of chemically produced excited states. J Am Chem Soc 94:7536–7541

9. Gundermann K-D, Drawert M (1962) Konstitution und Chem-ilumineszenz, I, Sterische Resonanzhinderung bei alkylierten Amino-Phthalhydraziden. Chem Ber 95:2018–2026

10. a) Neumann H, Jacobi von Wangelin A, Gördes D, Spannenberg A, Beller M (2001) A new multicomponent coupling of aldehydes, amides, and dienophiles: Atom-efficient one-pot synthesis of highly substituted cyclohexenes and cyclohexadienes. J Am Chem Soc 123:8398–8399. b) Jacobi von Wangelin A, Neumann H, Gördes D, Spannenberg A, Beller M (2001) Facile three-component coupling procedure for the synthesis of substi-tuted tetrahydroisoindole-1,3-diones from α,β-unsaturated alde-hydes. Org Lett 3:2895–2898. c) Klaus S, Hübner S, Neumann H, Strübing D, Jacobi von Wangelin A, Gördes D, Beller M (2004) Second generation protocol for multicomponent coupling reac-tions of aldehydes, amides and dienophiles. Adv Synth Catal 346:970–978. d) Neumann H, Jacobi von Wangelin A, Klaus S, Strübing D, Gördes D, Beller M (2003) Anilines made easily: From aldehydes to tri-, tetra-, and pentasubstituted anilines in two steps. Angew Chem Int Ed 42:4503–4507. e) Neumann H, Klaus S, Klawonn M, Strübing D, Hübner S, Gördes D, Jacobi von Wangelin A, Lalk M, Beller M (2004) A new efficient synthesis of substituted luminols using multicomponent reactions. Z Naturforsch 59b:431–438

11. a) Jacobi von Wangelin A, Neumann H, Gördes D, Klaus S, Strübing D, Beller M (2003) Multicomponent coupling reactions for organic synthesis: chemoselective reactions with amide-aldehyde mixtures. Chem Eur J 9:4286–4294. b) Strübing D, Jacobi von Wangelin A, Neumann H, Gördes D, Hübner S, Klaus S, Spannenberg A, Beller M (2005) Multicomponent reaction of aldehydes, anhydrides, and dienophiles: synthesis of "butterfly"-like diazatetradecenes. Eur J Org Chem 107–113. c) Strübing D, Neumann H, Klaus S, Jacobi von Wangelin A, Gördes D, Beller M, Braiuca P, Ebert C, Gardossi L, Kragl U (2004) Enzymatic resolution of 4-N-phenylacetylamino-derivatives obtained from multicomponent reactions using PenG amidase and in silico studies. Tetrahedron 60:683–691. d) Jacobi von Wangelin A, Neumann H, Gördes D, Hübner S, Wendler C, Klaus S, Strübing D, Spannenberg A, Jiao H, El Firdoussi L, Thurow K, Stoll N, Beller M (2005) Sequential three-component and Heck reactions for the synthesis of phenanthridones. Synthesis 12:2029–2038

12. Becke AD (1993) Density-functional thermochemistry. III. The role of exact exchange. J Chem Phys 98:5648–5652

13. a) Lee C, Yang W, Parr RG (1988) Development of the Colle-Salvetti correlation-energy formula into a functional of the electron density. Phys Rev B 37:785–789. b) Miehlich B, Savin A, Stoll H, Preuss H (1989) Results obtained with the correlation energy density functionals of Becke and Lee, Yang and Parr. Chem Phys Lett 157:200–206

14. a) McLean AD, Chandler GS (1980) Contracted Gaussian basis sets for molecular calculations. I. Second row atoms, z=11–18. J Chem Phys 72:5639–5648. b) Krishnan R, Binkley JS, Seeger R, Pople JA (1980) Self-consistent molecular orbital methods. XX. A basis set for correlated wave-functions. J Chem Phys 72:650–654

15. Frisch MJ, Trucks GW, Schlegel HB, Scuseria GE, Robb MA, Cheeseman JR, Montgomery JA Jr, Vreven T, Kudin KN, Burant JC, Millam JM, Iyengar SS, Tomasi J, Barone V, Mennucci B, Cossi M, Scalmani G, Rega N, Petersson GA, Nakatsuji H, Hada M, Ehara M, Toyota K, Fukuda R, Hasegawa J, Ishida M, Nakajima T, Honda Y, Kitao O, Nakai H, Klene M, Li X, Knox JE, Hrahian HP, Cross JB, Bakken V, Adamo C, Jaramillo J, Gomperts R, Stratmann RE, Yazyev O, Austin AJ, Cammi R, Pomelli C, Ochterski JW, Ayala PY, Morokuma K, Voth GA, Salvador P, Dannenberg JJ, Zakrzewski VG, Dapprich S, Daniels AD, Strain MC, Farkas O, Malick DK, Rabuck AD, Raghavachari K, Foresman JB, Ortiz JV, Cui Q, Baboul AG, Clifford S, Cioslowski J, Stefanov BB, Liu G, Liashenko A, Piskorz P, Komaromi I, Martin RL, Fox DJ, Keith T, Al-Laham MA, Peng CY, Nanayakkara A, Challacombe M, Gill PMW, Johnson B, Chen W, Wong MW, Gonzalez C, Pople JA. Gaussian 03, Revision D.02, (2004) Gaussian Inc., Wallingford, CT

16. a) Amovilli C, Barone V, Cammi R, Cancès E, Cossi M, Mennucci B, Pomelli CS, Tomasi J (1999) Advances in Quantum Chemistry, Vol 32: Quantum Systems in Chemistry and Physics, Part II. Academic Press, San Diego, USA, pp 227. b) Tomasi J, Cammi R, Mennucci B, Cappelli C, Corni S (2002) Molecular properties in solution described with a continuum solvation model. Phys Chem Chem Phys 4:5697–5712

17. a) Stratmann RE, Scuseria GE, Frisch MJ (1998) An efficient implementation of time-dependent density-functional theory for the calculation of excitation energies of large molecules. J Chem Phys 109:8218–8224. b) Bauernschmitt R, Ahlrichs R (1996) Treatment of electronic excitations within the adiabatic approxi-mation of time dependent density functional theory. Chem Phys Lett 256:454–464. c) Casida ME, Jamorski C, Casida KC, Salahub DR (1998) Molecular excitation energies to high-lying bound states from time-dependent density-functional response theory: Characterization and correction of the time-dependent local density approximation ionization threshold. J Chem Phys 108:4439–4449

18. Ghoneim N (1991) Solvatochromic spectroscopy of luminol in solvent mixtures. J Photochem Photobiol A: Chem 60:175–182

19. Zhao Y, Bordwell FG, Cheng J-P, Wang D (1997) Equilibrium acidities and homolytic bond dissociation energies (BDEs) of the acidic H-N bonds in hydrazines and hydrazides. J Am Chem Soc 119:9125–9129

20. Blunk D, Griesbeck AG, Jacobi von Wangelin A, unpublished results